ELSEVIER

Ultrasonics 34 (1996) 661–667

Ultrasonics

Comparison of the abilities of eight acoustic techniques to detect and size a single bubble

T.G. Leighton, A.D. Phelps *, D.G. Ramble, D.A. Sharpe

Institute of Sound & Vibration Research, Southampton University, Highfield, Southampton SO17 1BJ, UK

Received 28 July 1995

Abstract

This paper details the preliminary results from the Characterisation Of Bubbles Using Simulataneous Techniques (COBUST). There are a range of acoustic techniques for characterising bubble populations within liquids. Each technique has limitations, and complete characterisation of a population requires the simultaneous use of several, so that the limitations of each find compensation in the others. Eight acoustic signals were scattered from a single bubble to determine how easily and accurately they can, individually or together, measure the bubble size.

Keywords: Bubble detection; Subharmonics; Cavitation

1. Introduction

Bubble detection is required for many industrial, medical and environmental applications [1,2]. The strong acoustic scattering properties of a bubble caused by the impedance mismatch at the wall make acoustic techniques particulary suitable for bubble sizing and, additionally, the pulsations of the bubble in a driving sound field have a well defined resonance frequency f_0, given by:

$$f_0 \approx \frac{1}{2\pi R_0}\sqrt{\frac{3\kappa p_0}{\rho}} \quad \text{(valid in water for } R_0 > 10\ \mu\text{m)}. \tag{1}$$

Here R_0 is the equilibrium radius, κ is the polytropic constant of the gas inside the bubble [3], p_0 is the hydrostatic pressure and ρ the liquid density. Thus, from a knowledge of the acoustic resonance frequency, the equilibrium radius can be readily determined.

The inherently nonlinear bubble pulsations tend to linearity at low amplitudes. These can be exploited through a number of possible measurement methods [3]. Historically, data collection investigating the linear response of a bubbly liquid at a particular frequency was assumed to be dominated by bubbles which were resonant with that frequency [4]. However, the acoustic scattering cross-section of this fundamental frequency is only a local, and not a global, maximum at resonance: bubbles very much larger than resonance size can geometrically scatter sound to a greater degree than smaller, resonant bubbles.

However, in general, nonlinear effects are associated with high amplitude pulsations, which in turn occur at the bubble's resonance. The simplest manifestation of this nonlinearity is the presence of harmonics at $2\omega_p$, $3\omega_p$ etc, of the pure tone driving frequency ω_p in the scattered signal. In the presence of non-resonant bubbles, a signal at ω_p alone is detected. This effect has previously been used to detect bubbles by looking for returned signals at twice the frequency of that of the driving sound field [5]. However, it has only been used for detecting bubbles of specific size using at most two different insonation frequencies. The emission of the second harmonic is a global maximum at resonance, although the signal can readily arise through non-bubble sources of nonlinearity [1], which must be carefully examined. Such sources do not include solid inhomogeneities.

A further refinement of the method for searching for these nonlinear pulsations involves two frequency

* Corresponding author. Fax: +44-(0)1703-593019; e-mail: ap@isvr.soton.ac.uk

PII S0041-624X(96)00053-4

insonation [6]. The applied sound field contains two frequencies: one an imaging signal at ω_i which is fixed and set much higher than the resonance frequencies of any bubbles under investigation; and the other, the pump signal ω_p, tuned to the resonance frequencies of any bubbles under investigation. At resonance the two frequencies will be nonlinearly coupled and generate sum-and-difference signals at $\omega_i \pm \omega_p$: in the presence of non-resonant bubbles, only ω_p and ω_i are detected. One advantage of combination-frequency methods is that the bubble resonance can generate a signal in the MHz range (close to ω_i), thereby shifting only nonlinearly mediated information away from 'masking' signals such as the acoustic input and ambient noise.

The aforementioned nonlinear techniques, while giving rise to a maximum signal strength around the bubble resonance, suffer in that sources other than resonant bubbles (e.g. turbulence, transducer effects etc) can, to a greater or lesser extent, generate the desired signal, indicating the presence of a resonant bubble when one is not present [7]. Such 'false triggering' has not to date been found when signals at $\omega_i \pm \omega_p/2$ are used for bubble sizing. These are caused by subharmonic oscillations of the resonant bubbles, and are generated when the amplitude of the insonating pump field exceeds the threshold value required to generate Faraday waves on the bubble surface [8].

Over this range of acoustic techniques by which bubble sizing can be achieved, there are inherent limitations: some techniques are appropriate only to relatively high, uniform, bubble population densities [9], where the inter-bubble spacing is very much less than the acoustic wavelength, allowing homogeneous bulk properties to be assigned to the 'bubbly liquid' as a whole; others may be practicable only at low densities [8]. Several are prone to false triggering, and to overcome this the techniques become considerably more complicated to deploy. It therefore would be desirable to be able to use a range of these techniques to simultaneously interrogate a given liquid sample. This would enable optimisation of the process of characterising the bubble population in the liquid with respect to minimising the ambiguity of the result and the complexity of the task, as the limitations of each technique can be compensated through the deployment of others. Since the ambiguities of each have been studied theoretically and experimentally [3], the emphasis of this study will be how successfully each technique can provide information about the simplest of controlled populations, that of a single stationary bubble.

2. Method

The single bubble used in the experiments was tethered to a wire, which was held in a rigid 'cage' configuration at the focus of the transducers. The frequency response of the apparatus was inverted by calibrating the equipment before experimentation with no bubbles present. This enabled the bubble to be insonated at equal pressure amplitudes when interrogated by a sequence of tonal pumping signals. The experimental set-up and data acquisition details can be found elsewhere [8,10].

The techniques which exploit the nonlinear bubble response at resonance must detect a signal at frequencies different to that of the driving signal. Therefore, the tests must be performed using discrete pumping signals, but the analysis of the received spectra as one insonates the bubble population with incremented pure tones (IPT) allows all the detection techniques to operate simultaneously. However, measurement of the linear backscatter will be at the same frequency as the pumping signal, and so there are no benefits from using sequential pure tones. Additionally, since only linear oscillations are required of the bubble to scatter the fundamental, the energy density invested in each frequency need not be high. Therefore, simultaneous investigation across a wide frequency range can be achieved using broadband insonation, in the form of band-limited white noise. Simultaneous analysis of the transfer function (i.e. output/input ratio) and coherence[1] between the returned and input signals can distinguish between bubbles and solid inhomogeneities, and indicate the approximate frequency range over which the more sophisticated but slower IPT techniques should subsequently be employed. The IPT tests were automated and optimised such that simultaneous measurement of the signals at ω_p, $2\omega_p$, $3\omega_p$, $\omega_i \pm \omega_p$, and $\omega_i \pm \omega_p/2$ at each setting of ω_p took about 0.4 s. In this way the techniques could be rapidly investigated to determine how far off resonance the insonating sound field must be before linear, harmonic and combination-frequency emissions from each bubble became negligible. During the experiment the bubble was imaged using a 3.5 MHz Hitachi EUB26 foetal scanner.

3. Results and discussion

The first results are shown in Fig. 1 for the broadband excitation. Fig. 1(a) illustrates the difference in the modulus of the voltage transfer function (the ratio of output to input) when the bubble was driven by a white noise signal band limited between 1 and 6 kHz. The response shows a rise in the signal with the bubble present at around 3500 Hz, followed by a sharp dip. This is the characteristic through-resonance behaviour of a bubble: just below resonance the bubble pulsations

[1] Both a bias in the estimation process due to a lack of frequency resolution and/or a nonlinearity may cause a dip in the coherence function.

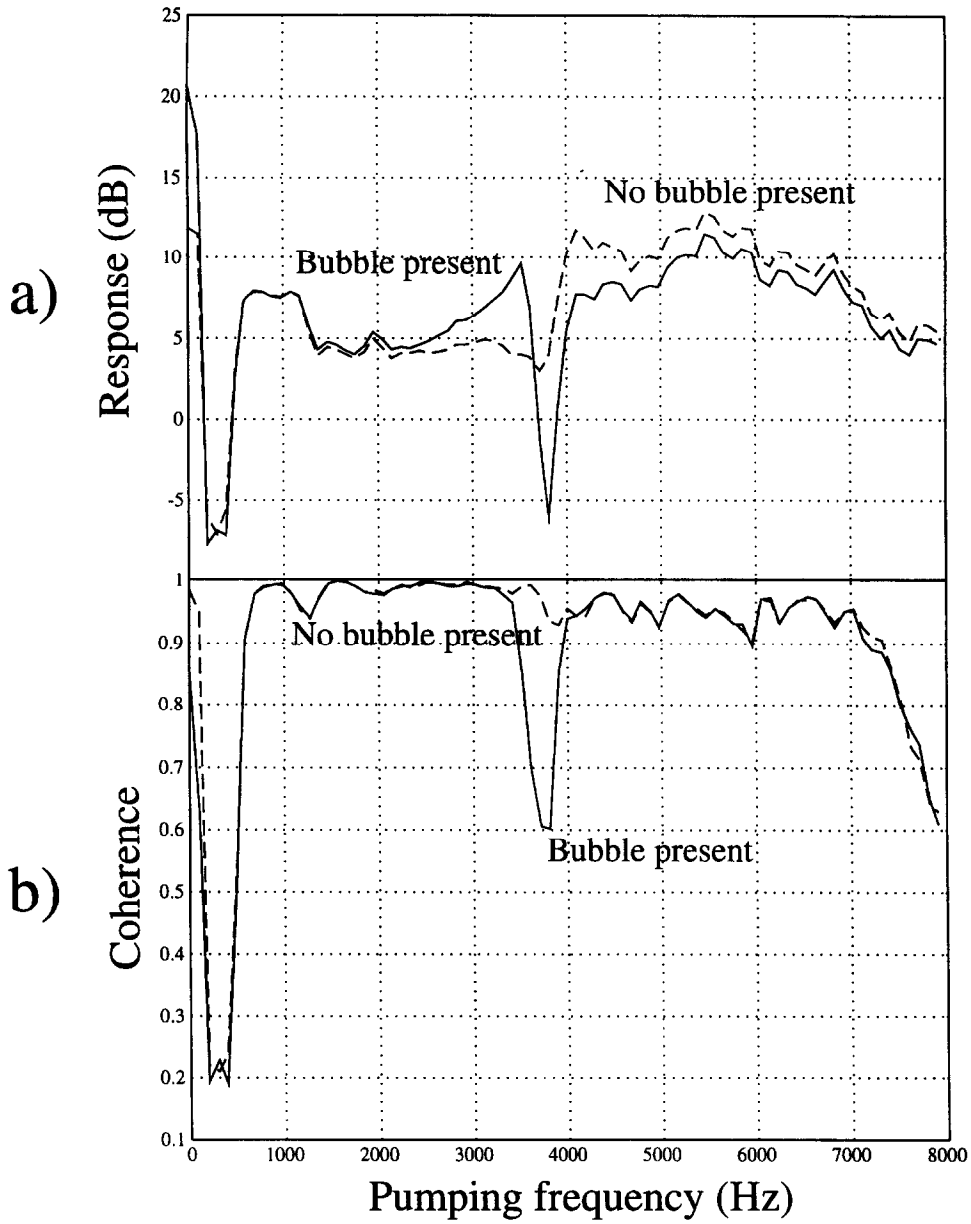

Fig. 1. Variation with frequency of (a) modulus of transfer function; and (b) coherence using 1–6 kHz band limited white noise, with a bubble present (unbroken) and with no bubble present (dashed). The data was averaged over 10 frames.

and the driving sound field are in phase and constructively interfere, but through resonance the bubble undergoes a π phase shift such that above resonance it pulsates in anti-phase with the sound field, resulting in destructive interference. That this occurs over a limited frequency range suggests that is does not represent geometric scattering from a large body, but is rather due to the presence of a bubble.

It is a drawback of the broadband excitation technique that the frequency response of the acoustic source and the tank cannot be compensated for, and so the rise in the signals above the bubble resonance may be misconstrued as positive signals. However, when the coherence between the signal input to the source and the returned signal is computed, such as that shown in Fig. 1(b), a definite bubble mediated reduction in the signal is evident. This technique does not suffer from the calibration problems present in the transfer function measurement.

These results immediately allow the range of interest for investigation of the harmonic and combination-frequency generation to be reduced to 1 kHz frequency span, which in this case was chosen as 3200–4200 Hz, incremented in 25 Hz steps. This was done at a pump signal pressure amplitude of 120 Pa. The results are given in Figs. 2 and 3 for the harmonic height and sum-and-difference heights respectively. The data are displayed as the heights of the signal at the frequency

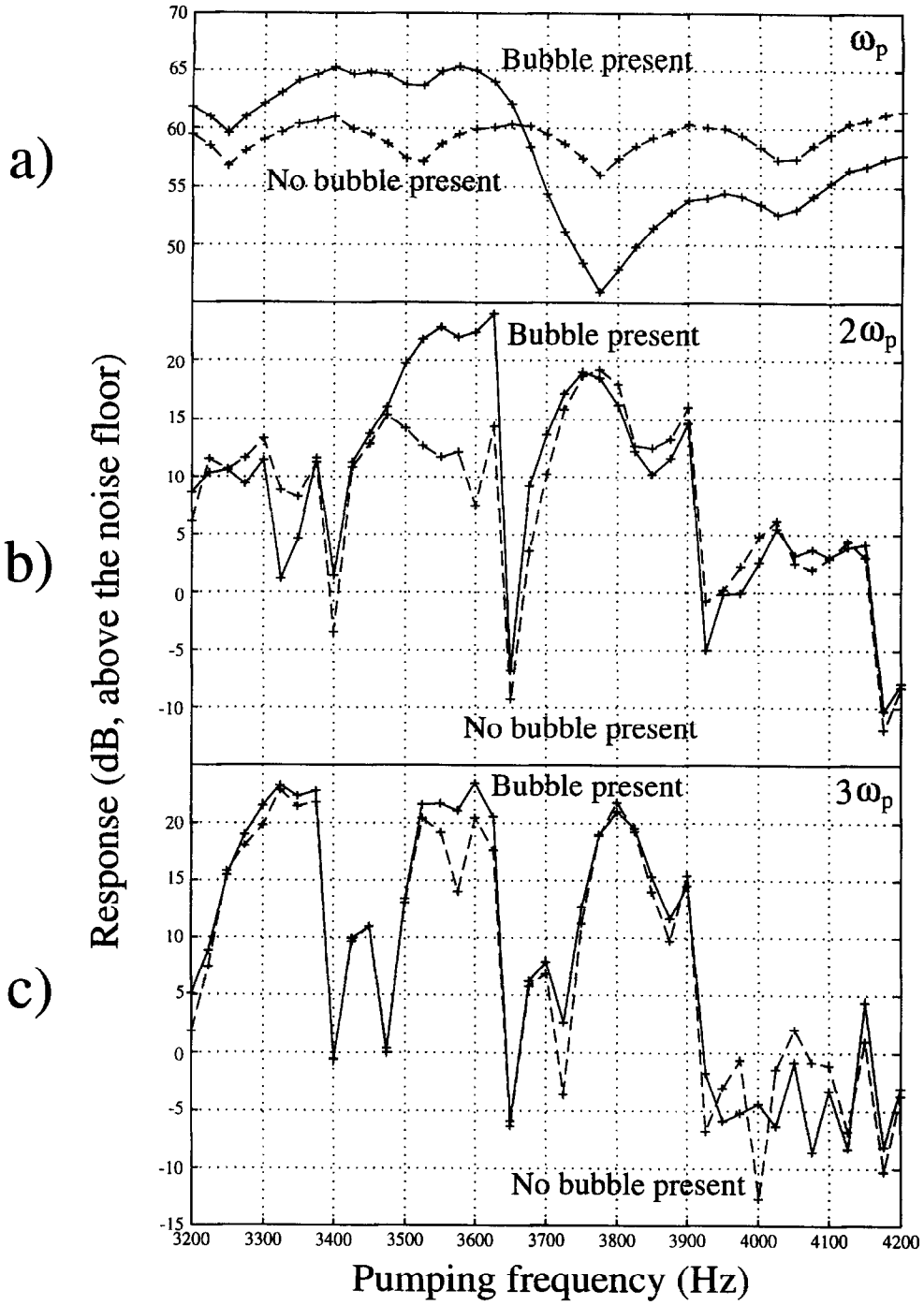

Fig. 2. Plot showing the variation with frequency of the (a) fundamental; (b) second harmonic; and (c) third harmonic of a bubble driven through its resonance in 25 Hz steps at 120 Pa excitation amplitude level (unbroken lines). The plots additionally show the heights of the signals with no bubble present (dashed).

locations of interest (i.e. ω_p, $2\omega_p$, $3\omega_p$, $\omega_i \pm \omega_p$ and $\omega_i \pm \omega_p/2$) for every incremented pump frequency. The data were sampled at 50 kHz and allowed a frequency resolution of 6 Hz. The imaging frequency was set at 1.1 MHz, and the $\omega_i \pm \omega_p$ and $\omega_i \pm \omega_p/2$ returned signals were heterodyned with this before sampling.

Fig. 2 shows the height of the backscattered fundamental, second harmonic and third harmonic signals. The fundamental backscatter, Fig. 2(a), shows a rippled amplitude response in the absence of a bubble, which is due to the differences in the proximity of each pumping signal tone to an FFT bin centre frequency. When the bubble was present, the characteristic rise and dip response is apparent, showing the presence of a resonant bubble at around 3600 Hz. The response of the second harmonic, in Fig. 2(b), is less clear. The height of the

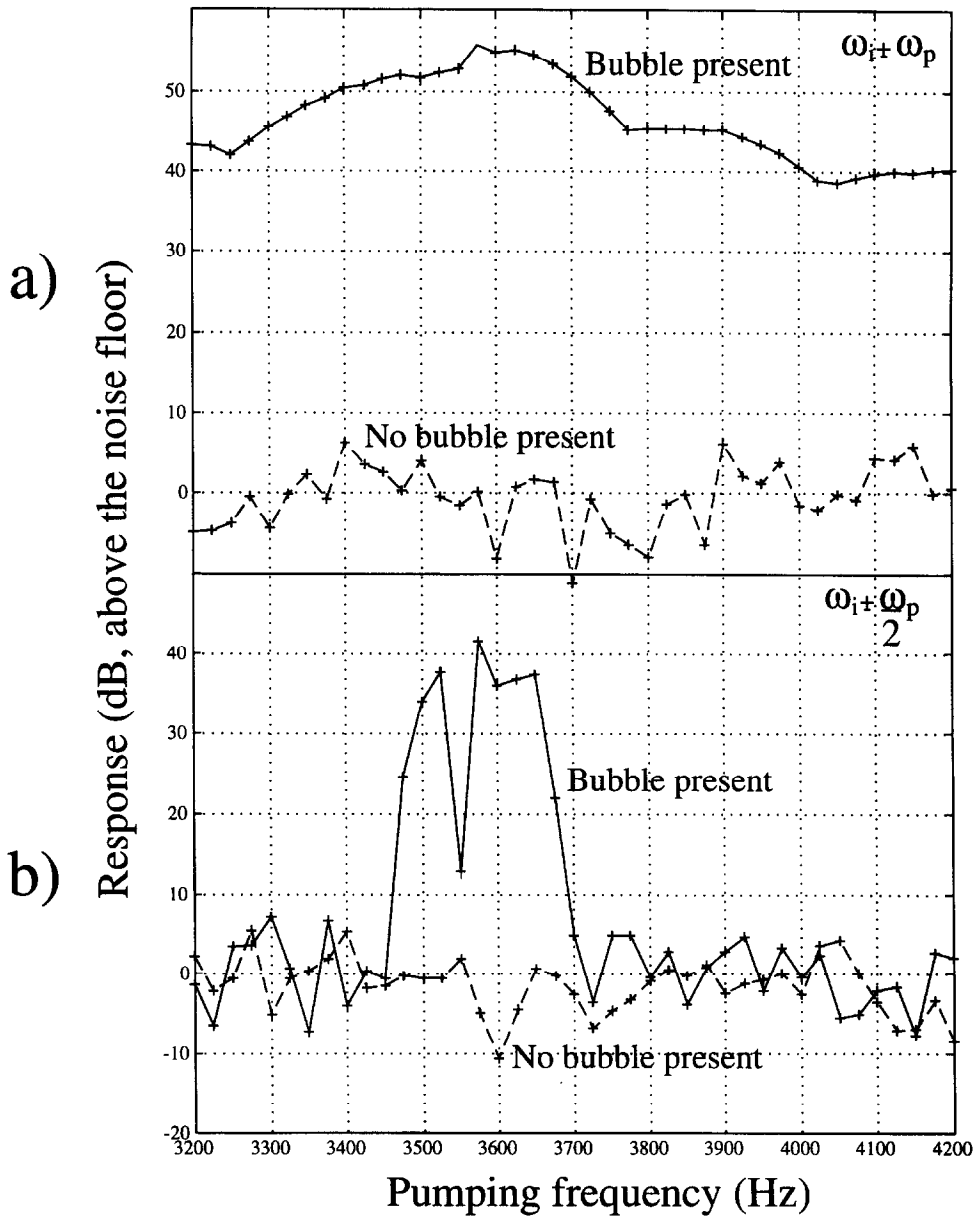

Fig. 3. Plot showing the variation with frequency of the (a) fundamental sum-and-difference; and (b) subharmonic sum-and-difference signals of a bubble driven through its resonance in 25 Hz steps at 120 Pa excitation amplitude level (unbroken lines). The plots additionally show the heights of the signals with no bubble present (dashed).

signal in the absence of the bubble is affected by many factors, including its proximity to a frequency bin and the relative levels of harmonic distortion in the equipment. However, a clear increase in the signal between 3500 and 3625 Hz is evident when the bubble was present. However, as it stands the harmonic output from the equipment must be very accurately known before experimentation to be able to make use of the bubble mediated signal in isolation. The data presented in Fig. 2(c) at the third harmonic of the driving signal shows very little change between the bubble present and the no bubble present data, and it would be fruitless to relate the amplitude of the signal to a bubble mediated effect. (If the high amplitude scattering is clipped, odd harmonics will be artificially enhanced.)

Fig. 3 shows the amplitude of the heterodyned returned signal from the high frequency transducer as a function of the incrementing pumping frequency ω_p at the speculative frequency location of the fundamental and subharmonic coupled signals. It is clear that the signal at $\omega_i \pm \omega_p$, which has been previously assumed to be an accurate measure of the resonance frequency [6,11], is present at around 40 dB above the noise floor over the entire pumping frequency span, and therefore provides a considerable off-resonance contribution to the returned signal. However, the coupled subharmonic signal at

Table 1
The various acoustic techniques available for bubble detection and the experimental results. The accuracy of each technique is determined as the frequency span over which a signal is returned which is less than 10 dB down on the height of the measured peak, and the maximum height is calculated as the maximum height of the bubble mediated signal above the non-bubble mediated signal.

Acoustic signal	Advantages	Disadvantages	Bubble resonance	Max height of signal	Accuracy (see note)
Broadband scattering (trans. fn. & coherence)	Apparatus simple. Distinguishes between bubbles and solid scatterers.	Difficult to invert measurement frequency response. Small signal increase at resonance.	3500 Hz	5 dB	Signal < 10 dB above background
Fundamental scattering	Apparatus simple.	Local maximum only, i.e. large bubbles and bubble clouds may falsely register as resonant bubble. Low spatial resolution. Small signal increase at resonance.	3575 Hz	5 dB	Signal < 10 dB above background.
Second harmonic	Global maximum at bubble resonance.	Low spatial resolution. Other sources of harmonic distortion will give a positive signal, so user must accurately know equipment harmonic distortion levels.	3550 Hz	9 dB	150 Hz
Third harmonic	Global maximum at bubble resonance.	No useful bubble mediated signal at this frequency location.	–	–	–
$\omega_i \pm \omega_p$	Moves bubble mediated information to low noise frequency location. Only nonlinearities in water will give false triggering.	Apparatus not simple. False triggering may occur from turbulence.	3575 Hz	55 dB	475 Hz
$\omega_i \pm \omega_p/2$	Unambiguous. Moves bubble mediated information to low noise frequency location.	Apparatus not simple. Threshold acoustic pressure required for fine resolution. Can only relate returned signal to one bubble.	3575 Hz	40 dB	150 Hz
Geometrical scattering using EUB26	Gives location through image	Poor sizing resolution (~0.5 mm)	Indicates location, but not size, of one bubble on wire		

$\omega_i \pm \omega_p/2$ exists only over a small frequency span with no off-resonance signal, and is thus unambiguously a measure of a resonant bubble.

The advantages, disadvantages and accuracy of each technique are presented in Table 1. The quoted accuracy of each technique is measured as the frequency span over which the returned signal is less than 10 dB down on the resonant value, and the maximum heights of the signals are calculated as the largest increases on the levels with no bubble present. The most accurate measurement for the resonance frequency of 3575 ± 75 Hz can be used to estimate the equilibrium bubble radius using Eq. (1) as 0.91 ± 0.02 mm. After experimentation the bubble was detached into a glass flask and measured optically [8], and the equivalent radius found to be 0.94 ± 0.05 mm.

4. Conclusions

Bubble population measurements can be more accurately taken using multiple acoustic techniques. First a broadband frequency signal can be employed to obtain an estimate of the bubble resonance locations, and these approximate frequency ranges can then be examined in detail using the simultaneous examination of five returned signals (ω_p, $2\omega_p$, $3\omega_p$, $\omega_i \pm \omega_p$, $\omega_i \pm \omega_p/2$). This incremented pure tone technique insonates the population at a constant pressure amplitude level, and thus comparison of these five signals will yield greater information on the population. The relative importance of each signal in determining the bubble population will be dependent on the population density and size, as the techniques which measure linear backscatter will be more applicable for high density populations, but for small numbers of bubbles more accurate and less ambiguous techniques may be used which relate the returned signal strength of the presence of individual members.

Acknowledgements

This work was funded by the Environmental and Physical Sciences Research Council, reference GR/H 79815.

References

[1] T.G. Leighton, J. Soc. Env. Eng. 7 (1994) 9.
[2] T.G. Leighton, J. Soc. Env. Eng. 8 (1995) 16.
[3] T.G. Leighton, The Acoustic Bubble (Academic Press, London, 1994).
[4] D.M. Farmer and S. Vagle, J. Acoust. Soc. Am. 86 (1989) 1897.
[5] D.L. Miller, A.R. Williams and D.R. Gross, Ultrasonics 22 (1984) 224.
[6] V.L. Newhouse and P.M. Shankar, J. Acoust. Soc. Am. 75 (1984) 1473.
[7] A.D. Phelps and T.G. Leighton, in: Proc. IUTAM Conf. on Bubble Dynamics and Interface Phenomena, Birmingham, 1993, Eds. J.R. Blake et al. (1994) 475.
[8] A. Phelps and T.G. Leighton, J. Acoust. Soc. Am. 99 (1995) 1985.
[9] N. Breitz and H. Medwin, J. Acoust. Soc. Am. 86 (1989) 739.
[10] A.D. Phelps and T.G. Leighton, in: Proc. 2nd European Conf. on Underwater Acoustics, Copenhagen, 1994, Ed. L. Bjorno (1994) 201.
[11] D. Koller, Y. Li, P.M. Shankar and V.L. Newhouse, IEEE J. Oceanic Engineering 17 (1992) 288.